Cooperative control method of seed and fertilizer simultaneous sowing of electric drive peanut planter

Yan Yu, Xiaomin Wang, Shuqi Shang*, Xiaozhi Tan, Dazhi Yi, Weikang Dong, Yushuai Song
(*College of Mechanical and Electrical Engineering, Qingdao Agricultural University, Qingdao 266109, China*)

Abstract: Aiming at the problems of low intelligence level of peanut seeder, unstable quality of sowing and fertilization, and poor coordination ability of one-time multi-work, this paper proposes a cooperative control method for simultaneous sowing and fertilization in electric-driven peanut planters. In this method, an improved cross-coupling control structure is proposed to realize the cooperative control of sowing and fertilization, and a fuzzy PID controller is designed. In addition, in order to solve the problem of high overshoot and poor system follow-up when the target speed of the control motor changes greatly during the operation process, an improved particle swarm optimization algorithm is introduced to reduce overshoot, improve response speed, and improve the control accuracy and stability of the seed and fertilizer simultaneous sowing control system. The method was simulated and analyzed on the Matlab/Simulink simulation platform, and the simulation results indicate that the dynamic performance and anti-interference capability of the improved controller have been significantly enhanced. To verify the effectiveness of this control method, an experiment on simultaneous sowing and fertilization of peanuts was designed. The experimental data showed that under stable operation, the average sowing qualification rate was 98.67% and the average fertilization qualification rate was 98.34%; under sudden load conditions, the average sowing qualification rate was 97.33% and the average fertilization qualification rate was 98.18%. The method maintained a low fluctuation range under different working conditions, effectively achieving precise simultaneous sowing and fertilization of peanuts. This research can provide an effective technical reference for efficient peanut cultivation.

Keywords: simultaneous sowing and fertilization, IPSO algorithm, improved cross-coupling structure, control system
DOI: 10.25165/j.ijabe.20251806.9547

Citation: Yu Y, Wang X M, Shang S Q, Tan X Z, Yi D Z, Dong W K, et al. Cooperative control method of seed and fertilizer simultaneous sowing of electric drive peanut planter. Int J Agric & Biol Eng, 2025; 18(6): 212–220.

1 Introduction

In modern agricultural production, improving the yield and quality of crops and reducing production costs has always been the focus of research by farmers and researchers. As one of the important economic crops in the world[1], peanut has rich nutritional value and wide market demand, and also occupies an important position in global agricultural production[2]. In the process of peanut planting, sowing and fertilization are the key links, which have a key impact on crop yield and quality. However, the traditional peanut planter generally has the problems of uneven sowing, unreasonable distribution of seed fertilizer, and low mechanical efficiency, which restricts the improvement of peanut yield and the efficient utilization of resources[3,4]. With the continuous development of agricultural intelligence, the application of electric drive system in agricultural machinery equipment is becoming more and more popular[5]. The introduction of electric drive technology provides the possibility of precise control for peanut sowing equipment. In order to solve the existing problems of peanut planting, this study aims to design a control method of seed and fertilizer simultaneous sowing of peanut planter based on motor drive technology to improve peanut planting efficiency.

In the study of simultaneous sowing of electric drive seed and fertilizer, the selection of control structure and control algorithm is the key to realizing the cooperative operation of high precision sowing and fertilization[6]. The goal of the control structure is to coordinate the sowing and fertilization module to achieve information interaction, improve the synchronization of sowing and fertilization, and adapt to the complex and changeable field environment. The control algorithm is to adjust the drive motor in real time by designing the seeding and fertilization controller to ensure the operation quality and equipment stability under different working conditions.

For the control structure, the current cooperative structure mainly includes parallel control, master-slave control, cross-coupling control, etc[7]. The parallel control structure has a wide range of applications, and because each control object has no influence on the others, this method is often used in scenarios with low accuracy requirements[8]. Compared with the parallel control structure, the master-slave control structure has better cooperative control performance, but there is a follow-up error, and the slave machine cannot be fed back to the host due to interference, which will have a negative impact on the final cooperative control effect[9,10].

Compared with the uncoupled control structure, the cross-coupled control structure has higher coordinated control

Received date: 2024-11-16 **Accepted date:** 2025-06-19
Biographies: Yan Yu, PhD, Professor, research interest: intelligent agricultural equipment, Email: 83518691@qq.com; **Xiaomin Wang**, MS candidate, research interest: agricultural electrification and automation, Email: 2298014546@qq.com; **Xiaozhi Tan**, MS candidate, research interest: agricultural electrification and automation, Email: 384461662@qq.com; **Dazhi Yi**, MS candidate, research interest: agricultural engineering and information technology, Email: 2406677654@qq.com; **Weikang Dong**, MS candidate, research interest: agricultural engineering and information technology, Email: 18354673839@163.com; **Yushuai Song**, MS candidate, research interest: agricultural machinery equipment engineering, Email: 1006213566@qq.com.
***Corresponding author: Shuqi Shang**, PhD, Professor, research interest: agricultural equipment design and theory. College of Electrical and Mechanical Engineering, Qingdao Agricultural University, Qingdao 266109, China. Tel: +86-13884956252, Email: sqshang@qau.edu.com.

performance. Because of its simple structure and good synchronization performance, it is widely used in dual-module synchronous control occasions[11].

For the control algorithm, some researchers have integrated intelligent algorithms such as fuzzy control, neural network, and sliding mode control into the control system. Li et al.[12] proposed a control scheme of sliding mode variable structure control. The sliding mode controller is used to control the space vector voltage, which effectively improves the static and dynamic performance of the system. However, the nonlinear characteristics of the sliding mode variable structure controller lead to the cumbersome tuning of the controller parameters, and the overall design process is too complicated.

Ma et al.[13] integrated the neural network algorithm into the two-axis coupling servo drive system, which effectively improved the synchronization performance between the motors. However, the neural network algorithm requires too much calculation and the system response speed is slow. Li et al.[14] used iterative optimization algorithm to optimize the structure and parameters of feedforward controller, which effectively improved the dynamic response characteristics of the system, but the static performance of the system needs to be improved. Si et al.[15] applied the variable universe fuzzy PI control algorithm to the speed loop of the brushless DC motor vector control system, and achieved good control results. Compared with other control algorithms, the fuzzy control algorithm does not need to accurately model the controlled object, and is suitable for dealing with nonlinear and uncertain problems in the motor control system[16,17].

To address the aforementioned issues, a cooperative control method for electric-driven simultaneous seeding and fertilization is designed. This method takes into account the operational requirements for peanut sowing and fertilization, proposing an improved cross-coupling control structure to enhance the synchronization of seeding and fertilization, developing a fuzzy PID controller, and introducing an improved particle swarm optimization algorithm to achieve stable output of the control motor, thereby improving the precision of the seeding and fertilization operations.

2 Composition of electric drive seeding and fertilization operation mechanism

2.1 Electric drive seed metering device

The electric drive peanut seed metering device is mainly composed of the seed metering device shell, the seed metering plate, the seed metering plate drive shaft, the deceleration device, the drive motor, the control system, and so on, as shown in Figure 1. The shell of the seed metering device mainly plays a protective role, providing a safe environment for peanut seeding, driving motor, and control system hardware; the seeding plate completes the seeding work; the driving shaft of the seed metering disc is responsible for transmitting the power of the driving motor to the seed metering disc and driving the seed metering disc to rotate. The role of the deceleration device is to amplify the torque of the drive motor; the brushless DC motor provides power for the seed metering device; the control system collects job information in real time and adjusts the job status online.

2.2 Electric drive fertilizer device

The electric drive fertilizer applicator is composed of an outer groove wheel fertilizer applicator, a deceleration mechanism, a DC brushless motor, a control system, etc., as shown in Figure 2. The brushless DC motor drives the fertilizer applicator through the deceleration mechanism, collects the operation information in real time through the system, and adjusts the speed of the brushless DC motor to control the fertilizer applicator for fertilization.

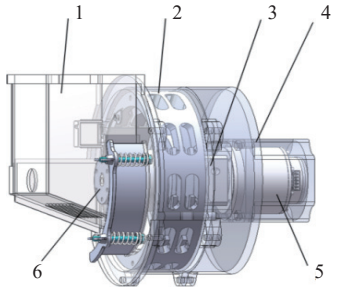

1. Seed inlet 2. Internal filling metering plate 3. Deceleration device 4. Seeding plate shell 5. DC brushless motor 6. Seeding plate drive shaft

Figure 1 Structure diagram of electric drive peanut seed metering device

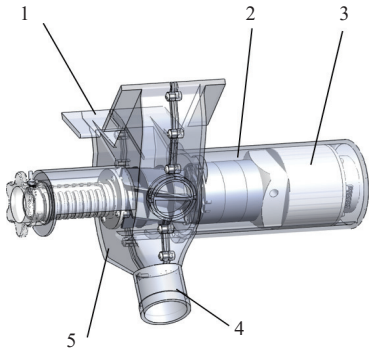

1. Fertilizer inlet 2. Deceleration device 3. DC brushless motor 4. Fertilizer outlet 5. Fertilizer shell

Figure 2 Structure diagram of electric drive peanut fertilizer applicator

3 Design of control structure for simultaneous sowing of seed and fertilizer

3.1 Mathematical model based on seed fertilizer application amount

For the seeding and fertilization system, the application amount of seed fertilizer can be expressed as the relationship between the speed output of the motor and the flow rate. The system controls the amount of seed and fertilizer application by controlling the motor speed, and the following relationship model can be established:

The amount of seed and fertilizer application can be expressed as:

$$Q_S = K_S N_{s1} \tag{1}$$

$$Q_f = K_f N_{s2} \tag{2}$$

where, Q_S is target application rate of seeds, kg/hm^2; Q_f is target application rate of fertilizer, kg/hm^2; N_{s1}, N_{s2} are the seeding motor speed and fertilization motor speed, r/min; K_S, K_f are application coefficient of seed and fertilizer, representing the proportional relationship between the motor speed and the amount of application, kg·min/r·hm^2.

$$Q_S : Q_f = \gamma \tag{3}$$

where, γ is the target application ratios of seeds and fertilizers. According to this ratio, the ideal relationship between the speed of the two motors can be obtained:

$$N_{s1}: N_{s2} = \gamma \cdot \frac{K_f}{K_S} = \alpha \tag{4}$$

In practical application, the application ratio of different seed fertilizers can be realized by adjusting the α value.

3.2 Dual-motor cross-coupling control structure model

The seeding module fertilization module is controlled by the motor alone, and the control instruction is sent to the motor through the microcontroller. If the control strategy is not adopted, there is no information interaction between the motors, which easily produces synchronization error, resulting in waste of resources[18,19]. By analyzing the structure of the electric drive peanut planter, combined with the requirements of sowing and fertilization, the common control strategies are studied and analyzed. The design of the seed and fertilizer simultaneous sowing system adopts the cross-coupling control strategy to form a communication closed-loop, correct the error, and realize the coordinated control of the motor. The cross-coupling control structure is shown in Figure 3.

The traditional cross-coupling control structure can only realize the synchronous control of the speed of the dual motor, but there are some limitations for speed proportional synchronization control, which cannot meet the dynamic adjustment demand of the application amount in the process of sowing and fertilization. In order to solve this problem, an improved cross-coupling control structure is proposed; that is, a speed proportional control module is added on the basis of the traditional cross-coupling control structure, and the system transmits the error of the two motors to ensure that the output of the two motors is consistent under various working conditions, so as to realize the simultaneous sowing of seed and fertilizer. The improved cross-coupling control structure is shown in Figure 4.

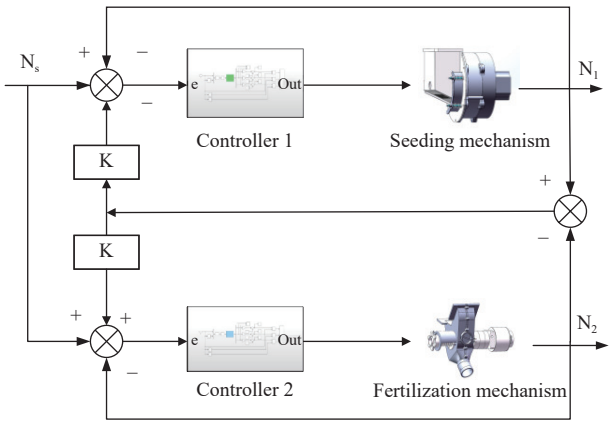

Figure 3 Cross-coupling control schematic diagram

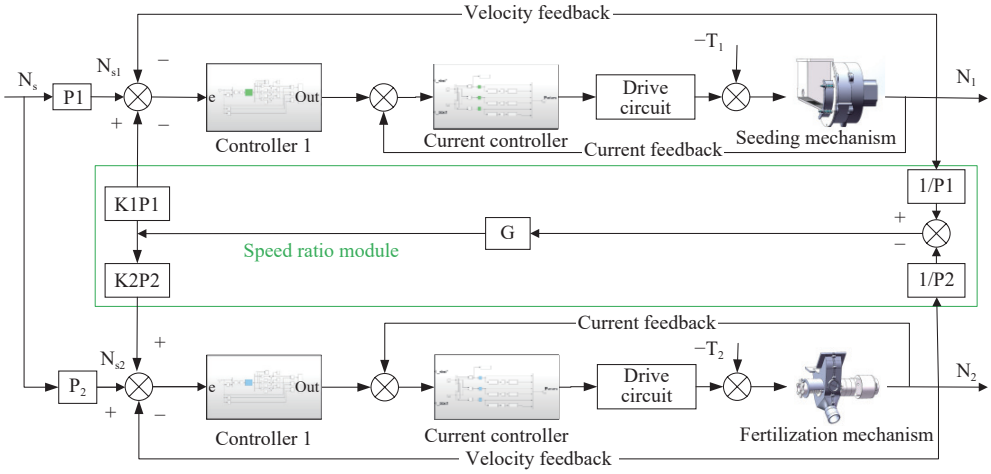

Note: P_i is speed proportional coefficient; K_i is synchronous coupling coefficient; T_i is load; G is synchronous control parameters; when two motors need to be controlled, set $G = 1$, and when only one motor needs to be controlled, set $G = 0$. While realizing the simultaneous sowing of seed and fertilizer, it also supports the separate operation of sowing and fertilization.

Figure 4 Improved cross-coupling control schematic diagram

Define the initial reference speed of the motor as N_s, and the theoretical speeds of the sowing and fertilizing motors as N_{s1}, N_{s2}, respectively:

$$N_{s1} = P_1 N_s \tag{5}$$

$$N_{s2} = P_2 N_s \tag{6}$$

Define the proportional tracking error of the sowing motor and the fertilizing motor as follows $E_1(t)$, $E_2(t)$:

$$E_1(t) = N_{s1} - N_1(t) \tag{7}$$

$$E_2(t) = N_{s2} - N_2(t) \tag{8}$$

where, $N_1(t)$, $N_2(t)$ represent the output speeds of the sowing motor and the fertilizing motor at time t.

$$\frac{P_1}{P_2} = \alpha \tag{9}$$

Define the proportional synchronization error of motor 1 and motor 2 as $H(t)$:

$$H(t) = \frac{N_1(t)}{P_1} - \frac{N_2(t)}{P_2} \tag{10}$$

Define the input of the seeding motor controller as $I_1(t)$ and the input of the fertilizing motor controller as $I_2(t)$:

$$I_1(t) = E_1(t) - GK_1P_1H(t) \tag{11}$$

$$I_2(t) = E_1(t) + GK_2P_2H(t) \tag{12}$$

4 Design of the control algorithm for simultaneous seeding and fertilization

4.1 Fuzzy PID controller design

Traditional PID controllers have fixed parameters, which limits their adaptability to complex and variable environments[20]. In contrast, fuzzy control algorithms do not rely on the mathematical model of the controlled object and exhibit strong adaptability to

changing conditions[21]. Therefore, this paper introduces fuzzy control algorithms to design a fuzzy PID controller to optimize control performance. The fuzzy PID controller consists of two parts: a fuzzy controller and a parameter-adjustable PID controller. The fuzzy controller takes the error e and the rate of change of error ec as inputs, and through fuzzification, fuzzy inference, and defuzzification, it obtains the adjustment amounts for the PID parameters ΔK_p, ΔK_i, and ΔK_d. Its structural block diagram is shown in Figure 5, where K_e and K_{ec} are quantization factors, and K_1, K_2, and K_3 are proportional factors.

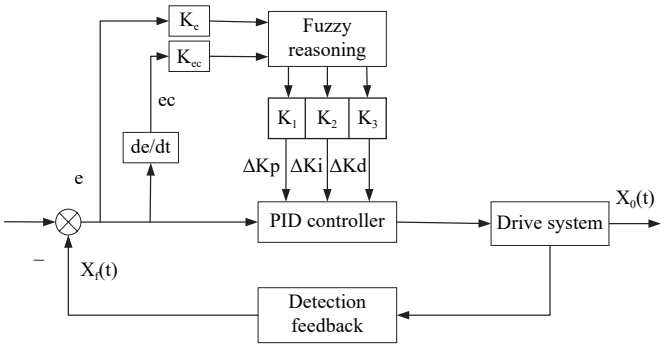

Figure 5 Fuzzy PID control structure diagram

For different e and ec, the PID parameters are adjusted based on fuzzy rules to meet the control requirements. The self-tuning PID parameters are calculated using the following equations:

$$K_p = K_{p0} + \Delta K_p \tag{13}$$

$$K_i = K_{i0} + \Delta K_i \tag{14}$$

$$K_d = K_{d0} + \Delta K_d \tag{15}$$

where, K_{p0}, K_{i0}, and K_{d0} are the initial values of the PID parameters; ΔK_p, ΔK_i, and ΔK_d are the outputs of the fuzzy control; K_p, K_i, and K_d are the final values of the control output parameters.

In Matlab, a fuzzy controller is established with input variables e and ec, and output variables ΔK_p, ΔK_i, and ΔK_d. The fuzzy subsets for all these variables are {Negative Big (NB), Negative Medium (NM), Negative Small (NS), Zero (ZO), Positive Small (PS), Positive Medium (PM), Positive Big (PB)}. Taking the seeding module as an example, the fuzzy domain for e and ec is (–6, 6), while the fuzzy domains for ΔK_p, ΔK_i, and ΔK_d are (–3, 3), (–0.6, 0.6), and (–3, 3), respectively.

Fuzzy rules are the foundation of a fuzzy controller and largely determine the control performance of the system. Based on expert experience and experimental analysis, the following fuzzy rules are established.

1) When the error e is large, a larger K_p value is selected to improve the system's response speed; a smaller K_i value or K_i is set to zero to avoid excessive overshoot and integral saturation; a smaller K_d value is chosen to prevent the instantaneous increase of the error from causing derivative overflow.

2) When the error e and the rate of change of error ec are of moderate size, the K_p value should be appropriately reduced to decrease the system's overshoot. At the same time, to ensure the stability of the system, the values of K_i and K_d should be moderate.

3) When the error e is small, larger values of K_p and K_i should be selected to improve system stability. At the same time, to enhance the system's ability to resist disturbances and avoid oscillations in the output response, when the rate of change of error ec is large, the K_d value should be set small; when ec is small, the K_d value should be set large.

According to the fuzzy control rules, a total of 49 rules have been formulated, focusing on tuning the three parameters: ΔK_p, ΔK_i, and ΔK_d. The fuzzy rule table is listed in Table 1. The visualization surface plot of the fuzzy rules is shown in Figure 6.

Table 1 Fuzzy rule table

$\Delta K_p/\Delta K_i/\Delta K_d$		*ec*						
		NB	NM	NS	ZO	PS	PM	PB
e	NB	PB/NB/PS	PB/NB/NS	PM/NM/NB	PM/NM/NB	PS/NS/NB	ZO/ZO/NM	ZO/ZO/PS
	NM	PB/NB/PS	PB/NB/NS	PM/NM/NB	PS/NS/NM	PS/NS/NM	NS/PS/NS	NS/ZO/ZO
	NS	PM/NB/ZO	PM/NM/NS	PM/NS/NM	PS/NS/NM	ZO/ZO/NB	NS/PS/NS	NS/PS/ZO
	Z	PM/NM/ZO	PM/NM/NS	PS/NS/NS	ZO/ZO/NS	NS/PS/NS	NM/PM/NS	NM/PM/ZO
	PS	PS/NM/NM	PS/NS/NS	ZO/ZO/ZO	NS/PS/PS	NM/PM/PM	NM/PM/PM	NM/PB/PB
	PM	PS/ZO/PB	ZO/ZO/PS	NS/PS/PS	NM/PS/PS	NM/PM/PS	NM/PB/PS	NB/PB/PB
	PB	ZO/ZO/PB	ZO/ZO/PM	NS/PS/PM	NM/PM/PM	NM/PM/PS	NM/PB/PS	NM/PB/PB

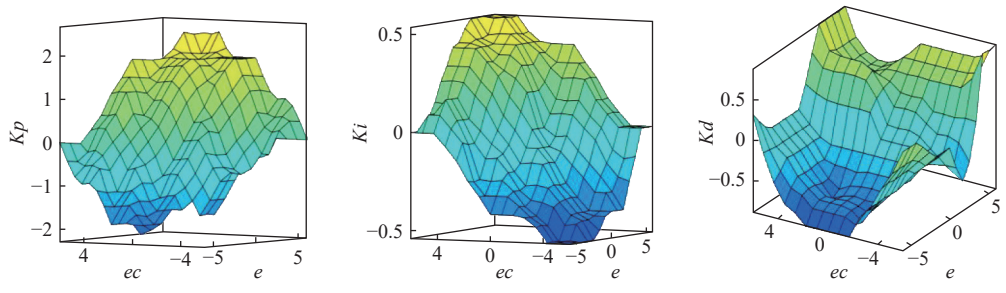

Figure 6 3D surface plot of fuzzy rules

Fuzzy control has limitations in adaptive capability and accuracy. Additionally, in fuzzy PID controllers, the quantization factors and proportional factors often require extensive time-consuming adjustments based on human experience, leading to significant randomness and making it difficult to determine the optimal controller parameters[22,23]. In this context, to optimize the quantization factors and proportional factors in the fuzzy controller, particle swarm optimization (PSO) is introduced to achieve the best adjustment of the parameters in the fuzzy controller, thereby realizing a more desirable control effect[24,25].

4.2 PSO

Particle Swarm Optimization algorithm is a typical swarm intelligence optimization algorithm[26]. Similar to most swarm intelligence optimization algorithms, this algorithm usually initializes a set of solutions (particles) randomly and then iteratively updates these solutions, allowing the entire population to adjust towards better fitness values. Ultimately, the goal is to find the optimal solution to the problem within a limited number of iterations[27]. The method for updating particle positions is shown in Figure 7.

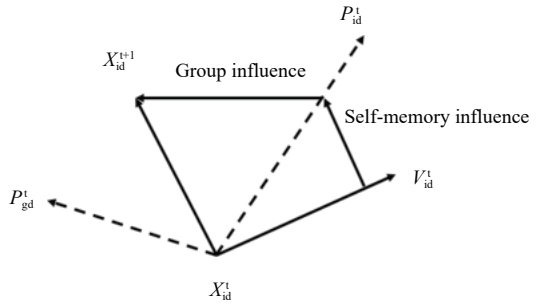

Figure 7 Particle position update method diagram

The corresponding velocity and position of the particle in space can be represented as:

$$V_{id}^{(t+1)} = WV_{id}^{(t)} + c_1 r_1 \left(p_{id}^{(t)} - X_{id}^{(t)}\right) + c_2 r_2 \left(p_{gd}^{(t)} - X_{id}^{(t)}\right) \tag{16}$$

$$X_{id}^{(t+1)} = X_{id}^{(t)} + V_{id}^{(t+1)} \tag{17}$$

where, V_i is the flying speed of particle i; X_i is the spatial position of particle i; $p_{id}^{(t)}$ and $p_{gd}^{(t)}$ are the individual optimal solution and global optimal solution at time t, respectively; c_1 and c_2 are learning factors; W is the inertia weight; d is the dimension of the decision variables; r_1 and r_2 are random numbers uniformly distributed between (0, 1); t_{max} and t are the maximum and current iteration counts, respectively.

After each iteration, the individual best solution of the particles needs to be updated according to the following rules:

$$P_i^{t+1} = \begin{cases} X_i^{t+1}, & f\left(X_i^{t+1}\right) < f\left(P_i^t\right) \\ P_i^t, & f\left(X_i^{t+1}\right) \gg f\left(P_i^t\right) \end{cases} \tag{18}$$

where, f(*) is the objective function for the fitness value at the corresponding position. The basic flow of the particle swarm optimization algorithm is shown in Figure 8.

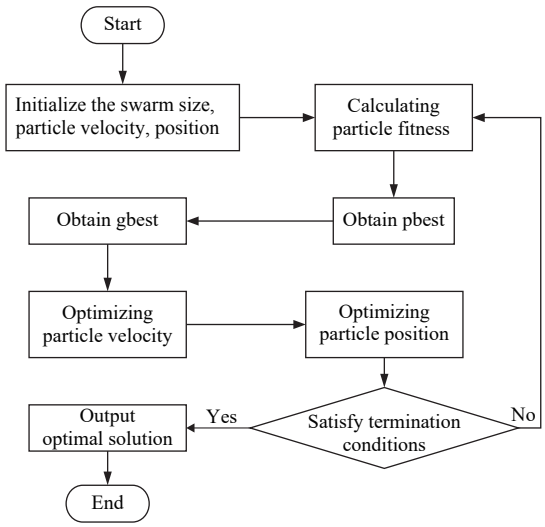

Figure 8 Flowchart of particle swarm optimization algorithm

4.3 Design of improved particle swarm optimization fuzzy PID controller

The traditional PSO algorithm is simple to operate and has strong versatility; however, it can sometimes easily get trapped in local optima, and its convergence speed significantly decreases in the later stages of evolution[28]. To improve the speed and accuracy of target parameter optimization and enhance the synchronization performance of the speed synchronization controller, the traditional PSO algorithm has been improved by incorporating adaptive dynamic inertia weight and particle mutation. The design method is as follows.

When the inertia weight of each particle decreases simply in a linear or nonlinear manner with the increase of iteration times, it can reduce the search accuracy. Therefore, based on this decrement, we consider the dynamic variation of the inertia weight value according to the position of the particles. Specifically, during the iterative evolution of the particles, when a particle's fitness value is greater than the average, we directly take the maximum inertia weight value to increase the search speed. When the fitness value of a particle is less than the average, the ratio of the distance of the individual particle to the optimal value to the average distance of all particles in the group to the optimal value is used as a nonlinear coefficient for adaptive dynamic adjustment[29]. The inertial weight value for nonlinear adaptive dynamic adjustment is determined as per the formula.

Adopting adaptive inertia weight:

$$W = \begin{cases} W_{\min} + \dfrac{(W_{\max} - W_{\min}) \times (f_i - f_{\min})}{f_a - f_{\min}}, & f_i \le f_a \\ W_{\max}, & f_i > f_a \end{cases} \tag{19}$$

where, f_i is the fitness value of the i-th particle; f_{min} and f_{avg} are the minimum and average fitness values of the particles at the current iteration, respectively; W_{max} and W_{min} are the maximum and minimum values of the inertia weight, respectively.

To address the issue of premature convergence in particle swarm optimization, which causes the search range of particles to shrink and makes it easy to get trapped in local optima, this paper introduces the following mutation rule:

$$X_{ib}^t = \begin{cases} X_{ib}^t \times (0.5\eta + 1), & r \gg C \\ X_{ib}^t, & r < C \end{cases} \tag{20}$$

where, X_{ib}^t represents the position of the i-th particle in the b-dimensional space after t iterations; η is a random variable that follows a Gaussian distribution in the range of [0, 1]; C is a value selected based on actual conditions. Although a good dynamic inertia weight can improve the accuracy and optimization speed of the algorithm, introducing particle mutation allows each particle in the population to have the opportunity to mutate during the iteration process, thereby enhancing the algorithm's global search capability.

Using the comprehensive evaluation index ITAE as the fitness function for the improved PSO[30], the quantization factor and proportional factor of the fuzzy PID controller are iteratively calculated, allowing the system's weighting factors to be quickly tuned. This not only reduces the dependence of the fuzzy controller on expert experience but also enables the control system to quickly reach a steady state, achieving intelligent adjustment of controller parameters[31]. The improved particle swarm algorithm process is shown in Figure 9.

$$J_{\mathrm{ITAE}} = \int_0^{\infty} t|e(t)|\mathrm{d}t \tag{21}$$

where, t is time and $e(t)$ is the error.

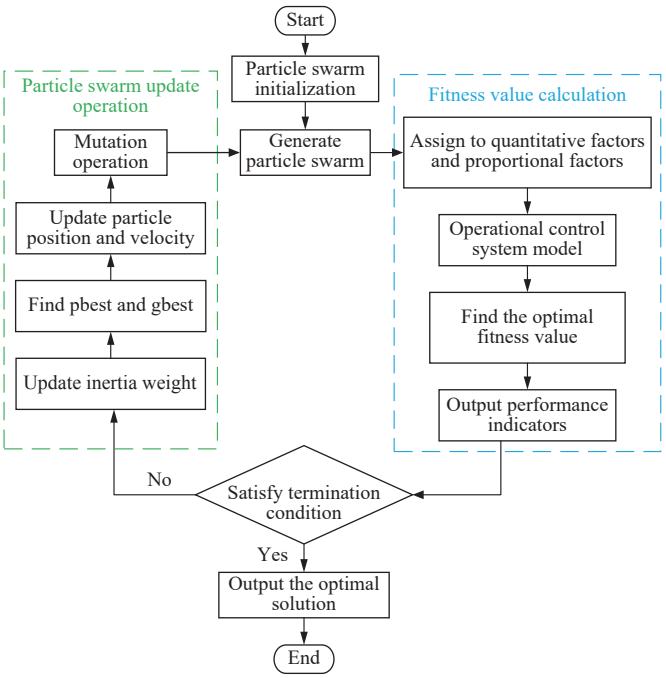

Figure 9 Flowchart of the improved particle swarm algorithm

5 Simulation experiment and analysis

5.1 Controller simulation experiment

To verify the performance of the improved particle swarm optimization fuzzy PID controller, a simulation model of the control system was established using the Simulink toolbox in Matlab to validate its effectiveness. In the Matlab/Simulink environment, a control system was built. To facilitate the comparison of the performance of different controllers, simulation models for fuzzy PID control, particle swarm fuzzy PID control, and improved particle swarm fuzzy PID control were established and analyzed comparatively, as shown in Figure 10.

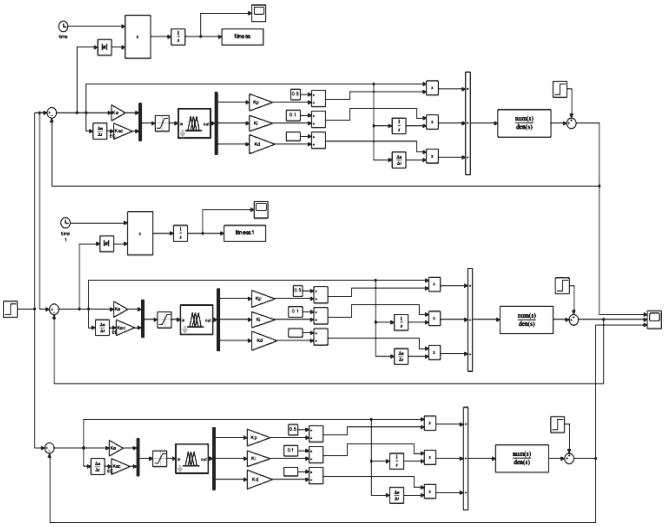

Figure 10 Controller simulation models

Set the number of particles $N = 100$, the maximum number of iterations $T = 50$, the inertia weight $W_{max} = 0.8$, $W_{min} = 0.3$, $c_1 = c_2 = 2$, $Dim = 5$.

To compare the iterative optimization capabilities of the algorithms before and after improvement, the fitness variation curve shown in Figure 11 was obtained.

According to the comparison of the fitness value evolution process, PSO shows little variation in fitness values after the 5th iteration, becoming trapped in a local optimum. In contrast, IPSO, due to the design of its dynamic nonlinear inertia weight curve that first convexes and then concaves, remains in a global optimization state until the 14th iteration, avoiding the situation of being stuck in a local optimum. Furthermore, from the 14th to the 18th iterations, it focuses on local optimization. The improved particle swarm optimization algorithm can significantly enhance the convergence rate of optimization while also promoting an increase in convergence accuracy.

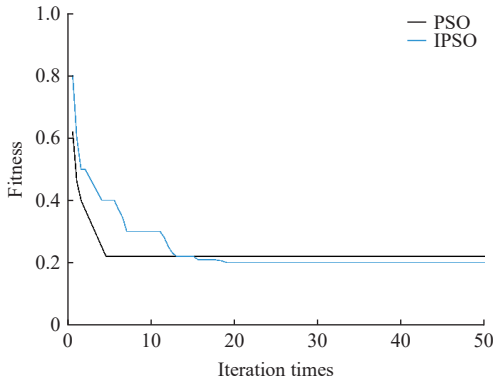

Figure 11 Fitness value variation curve

To comprehensively evaluate the performance of the controller, a step signal is set as the system input, and the response curves of different controllers are compared. After introducing the particle swarm optimization, the response curve shows no overshoot, and the improved particle swarm algorithm further enhances the response speed. The comparison of the response curves is shown in Figure 12, and the comparison of performance parameters is listed in Table 2.

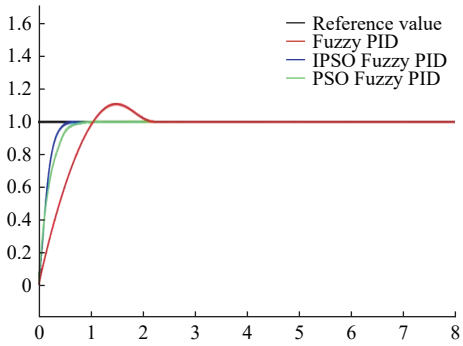

Figure 12 Comparison of response curves

Table 2 System performance parameters

Parameter	Fuzzy-PID	PSO-Fuzzy-PID	IPSO-Fuzzy-PID
Rise time/s	1.1	0.47	0.37
Overshoot/%	15	0	0
Settling time/s	2.1	0.8	0.6

To test the system's anti-interference performance, interference signals are introduced during the simulation process to compare the anti-interference capabilities of different controllers. The response curve to the introduced interference signal is shown in Figure 13.

A disturbance signal was introduced at 4 seconds, and the response time of the IPSO-Fuzzy-PID controller was significantly shortened, allowing the system to quickly return to a steady state. The results indicate that by improving the particle swarm algorithm, both the dynamic performance and the anti-interference capability of the controller have been significantly enhanced.

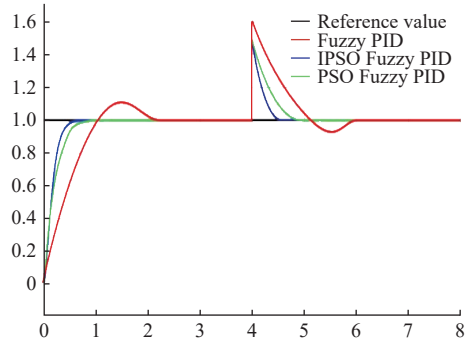

Figure 13 Comparison of response curves to sudden disturbances

5.2 Simulation and analysis of motor speed synchronous control

In the Matlab/Simulink simulation environment, an improved cross-coupling synchronous control simulation model is established, as shown in Figure 14.

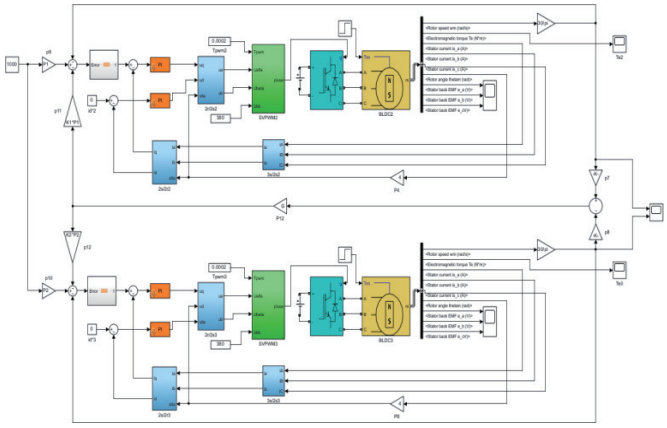

Figure 14 Simulation diagram of improved cross-coupling control structure

The motor model parameters for the seeding and fertilizing operation are as follows: rotational inertia J=0.002 218 kg·m^2, system friction is ignored, the electric angle of the trapezoidal wave induced electromotive force flat-top region is 120°, stator phase winding resistance R_S=0.0261 Ω, stator phase winding inductance L=6.77×10^{-3} H, and torque constant K_T=0.2361 N·m/A. A particle swarm optimization fuzzy PID controller is used to compare the speed errors of the two motors under parallel control, master-slave control, and improved cross-coupling control structures to verify the synchronization of the control system.

When the two motors are connected using a parallel strategy, they initially exhibit good cooperation. However, after a disturbance is introduced, the speed of Motor 1 begins to fluctuate, while Motor 2 continues to operate according to its original pattern. There is no information exchange between the two, leading to an increasing cooperative error that varies with the disturbance. When the two motors are connected using a master-slave strategy, there is a significant lag in the response of the slave motor. After the master motor is disturbed, this disturbance is transmitted to the slave motor, causing its speed to also begin to fluctuate. As a result, the cooperative error between the motors is relatively large in the initial phase. However, as the response of the slave motor gradually decreases, the cooperative error subsequently varies with the disturbance. When the two motors are connected using an improved cross-coupling strategy, the cross-coupling controller can adjust the control parameters in real time based on the feedback information from each motor. As a result, the response performance of the motors is optimal, and the cooperative error between the two motors is minimized. After Motor 1 is disturbed, it can quickly adjust, keeping the cooperative error at a minimum. The cooperative error of the dual motors is shown in Figure 15.

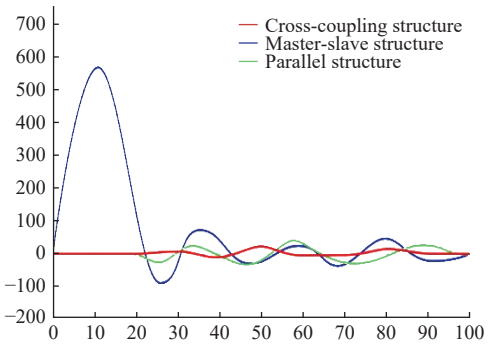

Figure 15 Cooperative error of dual motors

6 Fertilizer and seed co-application experiment

To verify the feasibility of applying this control method in the co-application of seed and fertilizer for peanut cultivation, a co-application experiment was conducted using an electric-driven seed dispenser and an electric-driven fertilizer dispenser is shown in Figure 16.

1. Seed dispensing motor 2. Electric drive peanut seed metering device 3. Platform lifting device 4. Fertilizer box 5. Electric-driven peanut fertilizer applicator 6. Fertilizer motor 7. Conveyor belt

Figure 16 Seed and fertilizer co-application experiment platform

The experimental parameter settings refer to the peanut sowing operation standards in Shandong Province. The operating speed is set at 3 km/h, the seed spacing is set at 20 cm, and the fertilization amount is set at 40 kg/667 m^2. By simulating the stable operation phase of the sowing machine and the load disturbance phase, the precision of seed and fertilizer co-application under parallel control, master-slave control, and improved cross-coupling control structures is compared to verify the effectiveness of the design method. Based on DB34/T 533-2022 “Technical Specifications for Mechanized Peanut Sowing Operations” and GB/T 20346.1-2021 “Fertilizer Machinery”, an experiment was conducted to determine the qualification rate of seed and fertilizer co-application.

In the seed and fertilizer co-application experiment, a sampling interval was established. Within this interval, the target seeding amount was set at 50 seeds and the target fertilization amount at 200 g. The actual number of seeds and the actual fertilization amount within the sampling interval were measured, and three experiments were conducted for each group.

As shown in Table 3, in the stable operation phase, both the parallel structure and the improved cross-coupling structure operation modes demonstrate a high precision in simultaneous sowing of seeds and fertilizers, with an average sowing compliance

rate exceeding 98% and an average fertilizer application compliance rate also exceeding 98%. However, under the master-slave control structure operation mode, due to communication delays and the influence of system response time, the fertilizer application compliance rate is around 94%.

Table 3 Results of the seed and fertilizer co-application experiment during the stable operation phase

Control structure	Seeding rate (seeds)	Seeding quality rate/%	Fertilizer application rate/g	Fertilization quality rate/%
Parallel structure	49	98	196.66	98.51
	50	100	203.76	98.12
	51	98	196.74	98.37
Master-slave structure	49	98	188.54	94.27
	49	98	187.72	93.86
	51	98	188.36	94.18
Improved cross-coupling structure	50	100	203.38	98.31
	51	98	196.44	98.22
	49	98	197.01	98.51

As shown in Table 4, when the sowing motor experiences a sudden load, in the parallel operational mode, there is no information interaction between the sowing module and the fertilization module, so the fertilization operation is unaffected, resulting in an average qualification rate of 98.31%. However, due to the load impact, the qualification rate for sowing significantly decreases, with an average qualification rate of 80.67%. In the master-slave control structure operational mode, the speeds of the sowing and fertilization motors are directly linked. Under the influence of load, the accuracy of both sowing and fertilization decreases simultaneously, resulting in an average sowing qualification rate of 80% and an average fertilization qualification rate of 76.99%. In the improved cross-coupling structure operational mode, under sudden load conditions, the speed ratio control module provides timely feedback on the generated speed synchronization errors. This allows for rapid adjustments to effectively reduce synchronization errors and stabilize output. The average sowing qualification rate is 97.33%, and the average fertilization qualification rate is 98.18%. Although these rates show a slight decrease compared to when the speed is stable, the reduction is within a low range, enabling effective precision sowing and fertilization of peanuts.

Table 4 Experimental results of simultaneous sowing of seeds and fertilizers under sudden load phase

Control structure	Seeding rate (seeds)	Seeding quality rate/%	Fertilizer application rate/g	Fertilization quality rate/%
Parallel structure	40	80	203.24	98.38
	39	78	203.86	98.07
	42	84	196.98	98.49
Master-slave structure	38	76	148.38	74.19
	42	84	160.62	80.31
	40	80	152.94	76.47
Improved cross-coupling structure	48	96	196.16	98.08
	49	98	196.58	98.29
	51	98	196.36	98.18

7 Conclusions

1) An improved cross-coupling control structure has been designed to dynamically adjust the sowing and fertilization amounts based on the working speed during peanut sowing and fertilization operations. A speed ratio control module has been added to the traditional cross-coupling control structure, allowing the sowing and fertilization motors to flexibly change their speeds and enhance the synchronization of sowing and fertilization.

2) A fuzzy PID controller has been designed, and the particle swarm optimization algorithm has been improved to further enhance the speed of parameter optimization and the anti-interference capability of the controller. This helps to avoid significant errors caused by disturbances during operation and the step change in target speed, thereby improving operational precision. Simulation analysis has verified that the improved controller effectively reduces overshoot, enhances response speed, and better meets the control requirements during sowing and fertilization operations, thus improving operational accuracy.

3) Using an electric drive peanut seed metering device and fertilizer applicator for testing, and combining an improved particle swarm optimization algorithm, the performance of parallel control, master-slave control, and improved cross-coupling control structures in peanut seed-fertilizer simultaneous sowing experiments was compared. It was concluded that the improved cross-coupling control structure excels in sowing accuracy and stability, making it more suitable for complex agricultural production environments.

This study enables the simultaneous implementation of precise peanut sowing and fertilization. By adopting this method, resource waste can be effectively reduced while also improving operational efficiency. It achieves fast broadcast and slow broadcast, ensuring uniform and consistent sowing rates, thereby meeting the goals of appropriate sowing and fertilization. It is hoped that this research will provide new solutions for sustainable agriculture and offer theoretical support and practical applications for electric-driven operations in agricultural machinery.

Acknowledgements

This work was financially supported by the National Key R&D Program Project (Grant No. 2023YFD2001002) and the Creation and Application of High-Quality, High-Efficiency Intelligent Peanut Sowing Technology and Equipment.

[References]

[1] Chen F D, Jiang J T, Wang D W, Bao Y F, Yang W Q. Application status and research progress of peanut planting machinery. Jiangsu Agricultural Science, 2020; 48(13): 41–46. (in Chinese)

[2] Zhang W L, Li X Z. The supply and demand situation of oilseed in china and strategies for capacity improvement. Journal of Chinese Farmers' Cooperatives, 2023; 10: 24–27. (in Chinese)

[3] Ren S H. Research on the control mechanism and monitoring system of electric drive air-suction precision corn seeding device. Heilongjiang Bayi Agricultural University, 2021. (in Chinese)

[4] Yao Y F. Design and research of electric drive seed discharge control system for high-speed precision corn planter. Shihezi University, 2023. (in Chinese)

[5] Hou Y T. Research and development of electric drive high-speed precision seeding technology. Agricultural Engineering, 2023; 35(4): 7–11.

[6] Xiao M H, Ma Y, Wang C, Chen J Y, Zhu Y J, Bartos P, et al. Design and experiment of fuzzy-PID based tillage depth control system for a self-propelled electric tiller. Int J Agric & Biol Eng, 2023; 16(4): 116–125.

[7] Liu R C. Research on synchronous control of multi-motor servo systems. Hangzhou: Zhejiang University, 2020. (in Chinese)

[8] Ye Y H, Peng F, Huang Y K. A review of multi-motor synchronous motion control technology. Transactions of China Electrotechnical Society, 2021; 36(14): 2922–2935.

[9] Liu F, Liu C, Rao H X, Xu Y, Huang T W. Reliable impulsive synchronization for fuzzy neural networks with mixed controllers. Neural

Networks, 2021; 143: 759–766.
[10] Basu H, Yoon Y. Cooperative output regulation of networked motors under switching communication and detectability constraints. IEEE Transactions on Control Systems Technology, 2020; 99: 1–8.
[11] Lu H, Fan W, Zhang Y Q, Ling H, Wang S J, Alghannam E, et al. Cross-coupled fuzzy logic sliding mode control of dual-driving feed system. Advances in Mechanical Engineering, 2018; 10(2): 1687814018755518. DOI: 10.1177/1687814018755518
[12] Li H Y, Ding S F, She C, Guo C J, Niu L L. Research on control of permanent magnet synchronous motors based on sliding mode variable structure. Foreign Electronic Measurement Technology, 2019; 38(9): 112–116. (in Chinese)
[13] Ma C, Jia C C. Motion control of dual-axis servo motors based on fuzzy neural networks. Electrical Drive, 2019; 49(9): 35–40. (in Chinese)
[14] Li S L, Duan S K, Li S L. Research on iterative optimization-based cross-coupling control method for multiple motors. Electrical Drive, 2021; 51(7): 46–51.
[15] Si L J, Huang Q L. Research on fuzzy PI control system with variable domain for brushless DC motors. Computer Simulation, 2020; 37(12): 214–218, 311.
[16] Wang X Y, Zhao J F. Design and implementation of PLC for dual motor synchronous control based on fuzzy PID. Modern Manufacturing Engineering, 2020; 10: 128–133.
[17] Jerković Š V, Varga T, Benšić T, Barukčić M. A survey of fuzzy algorithms used in multi-motor systems control. Electronics, 2020; 9(11): 1788.
[18] Zhang Q. Research on the problem of multi-motor synchronous control. Master's thesis, Harbin Institute of Technology, 2016. (in Chinese)
[19] Cui M K. Research on topology and control strategy of dual-winding permanent magnet synchronous motor system. Harbin Institute of Technology, 2022. (in Chinese)
[20] Zhao Z Z, Zhang G Z, Luo C M, Liu W R, Tang N R, Kang Q X, et al. Path tracking algorithm for dual-motor tracked chassis considering slip and skid. Transactions of the CSAE, 2024; 40(12): 46–54. (in Chinese)
[21] Gu X. Research on multi-motor collaborative control method based on intelligent optimization algorithms. Master's thesis, Changchun University of Technology, 2022. (in Chinese)
[22] Yu Y, Hu Y R, Shang S Q, Diao L S, Ge R C, Zhang X. Design of motor-driven precision seed-metering device with improved fuzzy PID controller for small peanut planters. Int J Agric & Biol Eng, 2023; 16(1): 136–144.
[23] Wang J H, Chen Y Z, Chen G, Lin J, Dai Z. Research on dual-motor synchronous control system based on cross-coupling control. Journal of Nanjing University of Science and Technology (Natural Science Edition), 2017; 41(6): 693–697. (in Chinese)
[24] Lu X, Ming L. A fuzzy logic controller tuned with improved PSO for delta robot trajectory control. Yokohama: IEEE Industrial Electronics Society, 2016.
[25] Li X Y, Xiao J, Pan Y P, Liu S Y, Deng X. Research on fuzzy pid control system for vehicle-borne platform leveling based on improved PSO. Modern Manufacturing Engineering, 2021; 2: 58–65. (in Chinese)
[26] Liu Z D, Hua L, Lyu Z Q, Hu J J, Zheng W X. Optimization and experimental analysis of sweet potato ship-shaped transplanting trajectory using particle swarm algorithm. Int J Agric & Biol Eng, 2024; 17(3): 100–107.
[27] Sousa-Ferreira I, Sousa D. A review of velocity-type PSO variants. Journal of Algorithms & Computational Technology, 2017; 11(1): 23–30.
[28] Wang Q Q, Li Z D, Wang W W, Zhang C L, Chen L Q, Wan L. Multi-objective optimization design of wheat centralized seed feeding device based on particle swarm optimization (PSO) algorithm. Int J Agric & Biol Eng, 2020; 13(6): 76–84.
[29] Zhou H F, Wang H W, Zhang Z J. Fuzzy identification of nonlinear systems based on adaptive particle swarm algorithm. Modern Electronic Technology, 2021; 44(10): 176–180.
[30] Afzal A, Ramis M K. Multi-objective optimization of thermal performance in battery system using genetic and particle swarm algorithm combined with fuzzy logics. The Journal of Energy Storage, 2020; 32(1): 101815.
[31] Chen Y N, Xie B, Du Y F, Mao E R. Powertrain parameter matching and optimal design of dual-motor driven electric tractor. Int J Agric & Biol Eng, 2019; 12(1): 33–41.